

# Dependence of Conductance on Percolation Backbone Mass

Gerald Paul,<sup>1\*</sup> Sergey V. Buldyrev,<sup>1</sup> Nikolay V. Dokholyan,<sup>1†</sup> Shlomo Havlin,<sup>2</sup>  
Peter R. King,<sup>3,4</sup> Youngki Lee,<sup>1</sup> and H. Eugene Stanley<sup>1</sup>

<sup>1</sup>*Center for Polymer Studies and Dept. of Physics, Boston University, Boston, MA 02215 USA*

<sup>2</sup>*Minerva Center and Department of Physics, Bar-Ilan University, Ramat Gan, Israel*

<sup>3</sup>*BP Amoco Exploration Operating Company Ltd., Sunbury-on-Thames, Middx., TW16 7LN, UK*

<sup>4</sup>*Department of Engineering, Cambridge University, Cambridge, UK*

(August 17, 2019)

On two-dimensional percolation clusters at the percolation threshold, we study  $\langle\sigma(M_B, r)\rangle$ , the average conductance of the backbone, defined by two points separated by Euclidean distance  $r$ , of mass  $M_B$ . We find that with increasing  $M_B$  and for fixed  $r$ ,  $\langle\sigma(M_B, r)\rangle$  asymptotically *decreases* to a constant, in contrast with the behavior of homogeneous systems and non-random fractals (such as the Sierpinski gasket) in which conductance increases with increasing  $M_B$ . We explain this behavior by studying the distribution of shortest paths between the two points on clusters with a given  $M_B$ . We also study the dependence of conductance on  $M_B$  slightly above the percolation threshold.

PACS numbers: 5.45.Df, 64.60.Ak, 64.60.Fr

## I. INTRODUCTION

There has been considerable study of the bond percolation cluster considered as a random-resistor network, with each occupied bond having unit resistance and non-occupied bonds having infinite resistance [1–3]. In two dimensions, the configuration studied is typically an  $L \times L$  lattice and the conductance is measured between two opposite sides which are assumed to have infinite conductance [4–16]. The backbone of the cluster is then defined as the set of bonds that are connected to the two sides having infinite conductance through paths that have no common bond.

At the percolation threshold, the backbone mass scales as  $\langle M_B \rangle \sim L^{d_B}$  with  $d_B = 1.6432 \pm 0.0008$  [17] and in this “bus bar” geometry is strongly correlated with  $L$ . The total conductance of the backbone as a function of  $L$  has been studied extensively and has been found to scale as  $\langle\sigma\rangle \sim L^{-\tilde{\mu}}$  with  $\tilde{\mu} = 0.9826 \pm 0.0008$  [17].

Recently, the distribution of masses of backbones defined by two *points*, i.e., backbones defined as the set of those bonds that are connected by paths having no common bonds to two points separated by distance  $r$  within an  $L \times L$  lattice, has been studied [18]. One finds that when  $r \ll L$ , there is a very broad distribution of backbone masses for a given  $r$ . Figure 1 illustrates some typical percolation clusters and their backbones defined in this configuration. Because of the broad distribution of backbone masses we have the opportunity to study the conductance between these two points separated by a fixed distance,  $r$ , as a function of the mass of the back-

bone defined by these points.

One might expect that, for fixed  $r$ , the average conductance would increase with increasing backbone mass because there could be more paths through which current can flow. In fact, we find that the average conductance decreases monotonically with increasing backbone size, in contrast with the behavior of homogeneous systems and non-random fractals in which conductance increases with increasing  $M_B$ . We explain our finding by noting that the conductance is strongly correlated with the shortest path between the two points, and then studying the distribution of shortest paths between the two points for a given  $M_B$ . This analysis extends recent studies of the distribution of shortest paths where no restriction on  $M_B$  is placed [19–22].

## II. SIMULATIONS

Our system is a two-dimensional square lattice of side  $L = 1000$  with points  $A$  and  $B$  defined as  $A = (L - r/2, 500)$ ,  $B = (L + r/2, 500)$ . For each realization of bond percolation on this lattice, if there is a path of connected bonds between  $A$  and  $B$ , we calculate (i) the length of the shortest path between  $A$  and  $B$ , (ii) the size of the backbone defined by  $A$  and  $B$  and (iii) the total conductance between  $A$  and  $B$ . We obtain data from 100,000 realizations for each of 8 values of  $r$  (1, 2, 4, 8, 16, 32, 64, and 128) at the percolation threshold,  $p_c = 0.5$ . We bin these results based on the value of the backbone mass,  $M_B$  by combining results for all realizations with

---

\*Electronic address: gerry@bu.edu

†Present address: Department of Chemistry and Chemical Biology, Harvard University, Cambridge, MA 02138 USA

$2^n < M_B < 2^{n+1}$  and taking the center of each bin as the value of  $M_B$ .

In Fig. 2(a), we plot the simulation results for the average conductance  $\langle \sigma(M_B, r) \rangle$  and find that the conductance, in fact, decreases with increasing  $M_B$ . The decrease is seen more clearly in Fig. 2(b), in which we plot scaled values as discussed below.

### III. SIERPINSKI GASKET

In non-fractal systems, the conductance increases as the mass of the conductor increases. We next consider the average conductance on the Sierpinski gasket, a non-random fractal, the first three generations of which are illustrated in Fig. 3(a)–(c). Because the Sierpinski gasket is not translationally invariant, the analogue of the average conductivity between two points in the percolation cluster is the conductivity averaged over all pairs of points separated by distance  $r$ . At each successive generation, there are two types of pairs: (i) pairs which correspond to pairs in the previous generation (e.g., A and B) and (ii) pairs which do not correspond to pairs in the previous generation (e.g., D and E). It is obvious that as we move from one generation to the next, the conductance between pairs of type (i) increases because there are more paths between the points than in the previous generation. On the other hand, the conductance between the pairs of type (ii) are lower on average than between the pairs present in the previous generation because on average the shortest path between the two points is longer than between the pairs in the previous generation. However, for any given  $r$ , the shortest path between any two points has a fixed upper bound independent of the generation. Due to this bound on the shortest path, the net result is that the average conductivity increases with succeeding generations. This is shown in Fig. 3(d) in which we plot the average conductivity calculated exactly for generations 1 to 6 for  $r = 1, 2$  and 4.

### IV. SHORTEST PATH DISTRIBUTION

In order to understand why the average conductance of the percolation backbone decreases with increasing  $M_B$ , we must (i) recognize that the conductance is strongly correlated with the shortest path between the two points and (ii) study  $P(\ell|M_B, r)$ , the distribution of shortest paths between the two points for a given backbone mass. Hence we next create the  $P(\ell|M_B, r)$  probability distribution, binning the data logarithmically by taking the average over samples centered at  $\log_2 \ell$ .

Figure 4(a) shows the results of the simulations for  $P(\ell|M_B, r)$  for  $r = 1$  for various backbone masses. The plots collapse, the only difference in the plots being the values of the upper cut-offs due to the finite size of the

backbone. Figure 1 illustrates how the size of the backbone constrains the possible values of the shortest path. For all values of  $M_B$ , a section of each plot in Fig. 4(a) exhibits power law behavior. In Fig. 4(b), we show the distributions  $P(\ell|M_B, r)$  for different  $r$  and a given  $M_B$ . In Fig. 4(c) we see that when scaled with  $r^{d_{\min}}$  the plots collapse, so we can write  $P(\ell|M_B, r)$  in the scaling form

$$P(\ell|M_B, r) \sim \frac{1}{r^{d_{\min}}} \left( \frac{\ell}{r^{d_{\min}}} \right)^{-\psi}. \quad (1)$$

An expression for  $\psi$  can be found by recognizing that we can write the well-studied distribution  $P(\ell|r)$ , the probability that the shortest path between two points separated by Euclidean distance  $r$  is  $\ell$ , independent of  $M_B$ , as

$$P(\ell|r) = \int_{c_\ell}^{\infty} P(\ell|M_B, r) P(M_B|r) dM_B, \quad (2)$$

where (i)  $P(M_B|r)$  is the distribution of backbone masses given distance  $r$  between the points which determine the backbone and (ii)  $c_\ell$  is the lower cutoff on  $M_B$  given  $\ell$ .  $P(M_B|r)$  has the form [18]

$$P(M_B|r) \sim \frac{1}{r^{d_B}} \left( \frac{M_B}{r^{d_B}} \right)^{-\tau_B}, \quad [r \ll L] \quad (3)$$

where  $d_B$  is the fractal dimension of the backbone and  $\tau_B = d/d_B$  is the exponent for the blob size distribution [1]. From Ref. [19]

$$P(\ell|r) \sim \frac{1}{r^{d_{\min}}} \left( \frac{\ell}{r^{d_{\min}}} \right)^{-g_\ell}, \quad (4)$$

where  $d_{\min}$  is the fractal dimension of the shortest path. Since  $\ell \sim r^{d_{\min}}$  and  $M_B \sim r^{d_B}$ , implying  $\ell \sim M_B^{d_{\min}/d_B}$ , the lower cutoff  $c_\ell$  in Eq. (2) scales as

$$c_\ell \sim \ell^{d_B/d_{\min}}. \quad (5)$$

As  $L \rightarrow \infty$ , the upper cutoff is  $\infty$  because the maximum backbone mass is not constrained by the length of the shortest path. Substituting Eqs. (3), (4), and (5) into Eq. (2), and equating powers of  $r$  (or powers of  $\ell$ ) of the left and right hand sides of the resulting equation, we find

$$\psi = g_\ell - \frac{d_B}{d_{\min}} (\tau_B - 1). \quad (6)$$

Using  $\tau_B = d/d_B$  and the values  $g_\ell = 2.04$  [19] and  $d_{\min} = 1.13$  [21], we find  $\psi = 1.72$ , in good agreement with our simulation result

$$\psi = 1.7 \pm 0.05. \quad (7)$$

## V. AVERAGE CONDUCTANCE

We can now calculate the average conductance. Since  $\sigma$  is strongly correlated with  $\ell$ , and since  $\sigma$  scales with  $r$  as  $r^{-\tilde{\mu}}$  and  $\ell$  scales with  $r$  as  $r^{d_{\min}}$ , we have

$$\langle \sigma \rangle \sim \ell^{-\tilde{\mu}/d_{\min}}. \quad (8)$$

Then using the fact that  $P(\ell|M_B, r) \sim \ell^{-\psi}$  we have

$$\begin{aligned} P(\sigma|M_B, r) &\sim P(\ell = \sigma^{-d_{\min}/\tilde{\mu}}|M_B, r) \frac{d\ell}{d\sigma} \\ &\sim \sigma^{(\psi-1)(d_{\min}/\tilde{\mu})-1} = \sigma^z, \end{aligned} \quad (9)$$

where

$$z \equiv (\psi - 1)(d_{\min}/\tilde{\mu}) - 1 = -0.17. \quad (10)$$

Now  $P(\ell|M_B, r)$  is nonzero only for

$$(ar)^{d_{\min}} \lesssim \ell \lesssim (bM_B)^{d_{\min}/d_B}, \quad (11)$$

where  $a$  and  $b$  are constants. Hence using  $\langle \sigma \rangle \sim \ell^{-\tilde{\mu}/d_{\min}}$ , we find  $P(\sigma|M_B, r)$  is nonzero for

$$(bM_B)^{(d_{\min}/d_B)(-\tilde{\mu}/d_{\min})} = (bM_B)^{-\tilde{\mu}/d_B} \lesssim \sigma \lesssim (ar)^{-\tilde{\mu}}. \quad (12)$$

Using these bounds to normalize the distribution, we find

$$P(\sigma|M_B, r) = \frac{(z+1)\sigma^z}{(ar)^{-\tilde{\mu}(z+1)} - (bM_B)^{(-\tilde{\mu}/d_B)(z+1)}}. \quad (13)$$

Then

$$\begin{aligned} \langle \sigma(M_B, r) \rangle &= \int_{(bM)^{-\tilde{\mu}/d_B}}^{(ar)^{-\tilde{\mu}}} \sigma P(\sigma|M_B, r) d\sigma \\ &= \frac{z+1}{z+2} (ar)^{-\tilde{\mu}} \frac{1 - \left[ \frac{(bM_B)^{1/d_B}}{ar} \right]^{-\tilde{\mu}(z+2)}}{1 - \left[ \frac{(bM_B)^{1/d_B}}{ar} \right]^{-\tilde{\mu}(z+1)}}. \end{aligned} \quad (14)$$

Thus as  $M_B$  goes to infinity,  $\langle \sigma(M_B, r) \rangle$  decreases asymptotically to a constant as

$$\langle \sigma(M_B, r) \rangle \sim \frac{z+1}{z+2} (ar)^{-\tilde{\mu}} \left[ 1 + \left[ \frac{(bM_B)^{1/d_B}}{ar} \right]^{-\tilde{\mu}(z+1)} \right]. \quad (15)$$

By considering the asymptotic dependence of  $\langle \sigma(M_B, r) \rangle$  on  $M_B$ , we can reasonably fit the simulation results by choosing the parameters  $a$  and  $b$  in Eq. (14) to be 0.9 and 6, respectively. Using these values for  $a$  and  $b$ , in Fig. 2(a) we plot  $\langle \sigma \rangle$  from Eq. (14) for multiple values of  $r$  and find that agreement with the simulation results improves with increasing  $r$ . For large  $r$ , the curves for the simulation results and the curves for the theoretical results are coincident at large  $M_B$ . The poor results for small  $r$  are due to

corrections-to-scaling not included in our derivation (e.g., for small  $r$ , there are significant corrections-to-scaling for the relations  $\sigma \sim r^{-\tilde{\mu}}$  and  $M_B \sim r^{d_B}$  [17]).

Equation (14) can be re-cast in terms of the scaled variable  $x \equiv M_B/r^{d_B}$  as

$$\sigma(x, r) = \frac{z+1}{z+2} (ar)^{-\tilde{\mu}} f(x), \quad (16)$$

where

$$f(x) = \frac{1 - \left( \frac{b}{a^{d_B}} x \right)^{-(\tilde{\mu}/d_B)(z+2)}}{1 - \left( \frac{b}{a^{d_B}} x \right)^{-(\tilde{\mu}/d_B)(z+1)}}. \quad (17)$$

In Fig. 2(b), we plot the average conductance scaled in accordance with Eqs. (16) and (17). The expected collapse improves with increasing  $r$  for the same reason as noted above.

Above the percolation threshold, for backbones of size larger than the correlation length, the strong correlation between the conductance and the shortest path breaks down and we expect the conductance to *increase* with the mass of the backbone, as is the case in non-random systems. This is seen in Fig. 2(c), where we plot conductance versus backbone mass for the bond occupation probabilities  $p = 0.56$  and  $p = 0.60$ , which are above the percolation threshold and, for comparison, conductance *at* the percolation threshold,  $p = 0.50$  [23]. Figure 2(c) shows that for  $p = 0.60$ , all backbone masses sampled are of size greater than the correlation length and the conductance increases monotonically. For  $p = 0.56$ , the smaller backbone masses are of size less than the correlation length and Fig. 2(c) shows that the conductance initially decreases; for larger backbone masses, however, the sizes of the backbones are greater than the correlation length and Fig. 2(c) shows that the conductance then increases.

## VI. DISCUSSION

The derivation of Eq. (14) and its agreement with the results of our simulations confirm our understanding of why the average conductance decreases with increasing backbone mass: the smaller contributions to the average conductance from the longer minimal paths possible in the clusters with larger backbone size cause the average conductance to be smaller. Our derivation was not specific to two dimensions, and should also hold in higher dimensions.

## ACKNOWLEDGMENTS

We thank J. Andrade for helpful discussions, and BP Amoco for financial support.

---

- [1] H. J. Herrmann, Phys. Reports **136**, 153 (1986).
- [2] T. Vicsek, *Fractal Growth Phenomena, 2nd Edition* (World Scientific Publishers, Singapore, 1992).
- [3] A. Bunde and S. Havlin (eds), *Fractals and Disordered Systems, 2nd Edition* (Springer, New York, 1996).
- [4] S. Alexander and R. Orbach, J. Phys. Lett. **43**, L625 (1982).
- [5] R. Pandey *et al.*, J. Stat. Phys. **34**, 427 (1984).
- [6] E. Duering and H. E. Roman, J. Stat. Phys. **64**, 851 (1991).
- [7] D. C. Hong *et al.*, Phys. Rev. B **30**, 4083 (1984).
- [8] B. Derrida and J. Vannimenus, J. Phys. A **15**, L557 (1982).
- [9] H. J. Herrmann *et al.*, Phys. Rev. B **30**, 4080 (1984).
- [10] J. M. Normand *et al.*, J. Stat. Phys. **52**, 441 (1988); Int. J. Mod. Phys. C **1** (1990).
- [11] R. Fogelholm, J. Phys. C. **13**, L571 (1980).
- [12] D. G. Gingold and C. J. Lobb, Phys. Rev. B **42**, 8220 (1990).
- [13] R. Fisch and A. B. Harris, Phys. Rev. B **18**, 416 (1978).
- [14] J. W. Essam and F. Bhatti, J. Phys. A **18**, 3577 (1985).
- [15] A. B. Harris and T. C. Lubensky, J. Phys. A **17**, L609 (1984).
- [16] A. Coniglio, M. Daoud and H. Herrmann, J. Phys. A **22**, 4189 (1989).
- [17] P. Grassberger, Physica A **262**, 251 (1999).
- [18] M. Barthélémy *et al.*, Phys. Rev. E **60**, R1123 (1999).
- [19] N.V. Dokholyan *et al.*, J. Stat. Phys. **93**, 603 (1998).
- [20] M. Porto *et al.*, Phys. Rev. E **58**, 5 (1998).
- [21] P. Grassberger, preprint cond-mat/9906309 (1999).
- [22] R. M. Ziff, preprint cond-mat/9907305 (1999).
- [23] Because, above the percolation threshold, the backbone mass is strongly correlated with the system size, we create backbones of a given mass by varying the system size. The simulations of Fig. 2(c) for the plots above the percolation were obtained choosing  $L = 6, 10, 20, 40, 80, 160,$  and  $200$ .

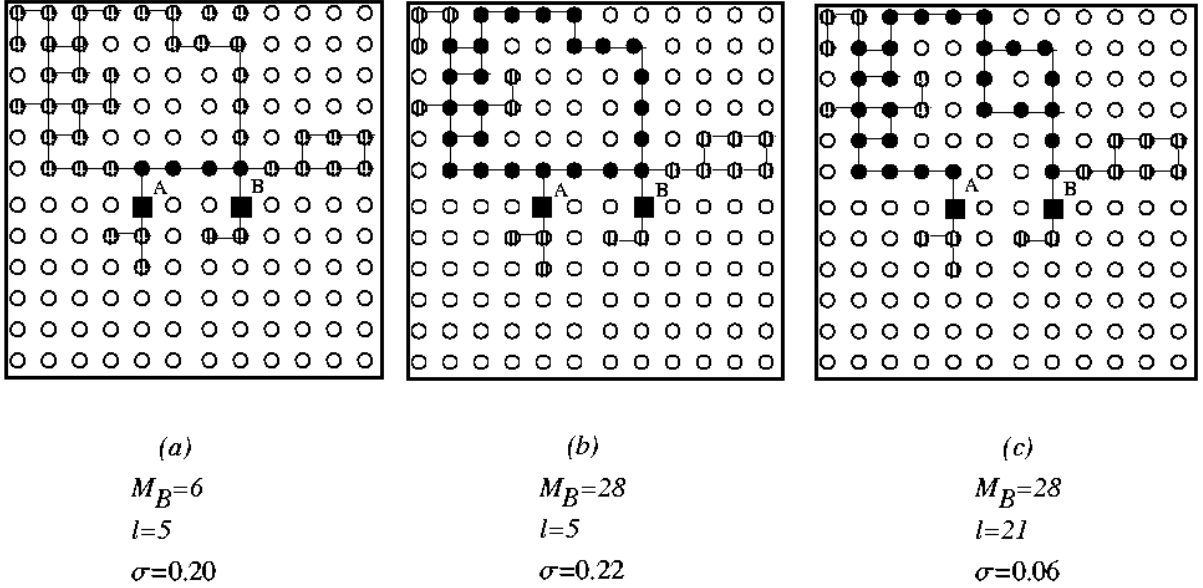


FIG. 1. Typical percolation clusters. The striped sites and the black sites are both part of the percolation cluster; only the black sites form the cluster backbone defined by sites  $A$  and  $B$  (black squares). Note in (a), with backbone size 6, the shortest path,  $\ell$ , between  $A$  and  $B$  is 5—the length of the shortest path must always be less than the backbone mass; (b) and (c) illustrate that in clusters with large backbones, the length of the shortest path between  $A$  and  $B$  can take on a broad range of values.

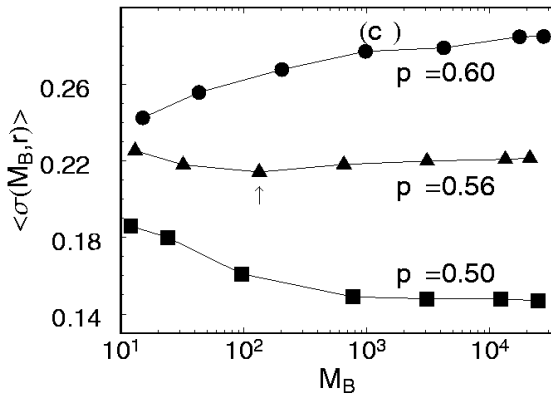
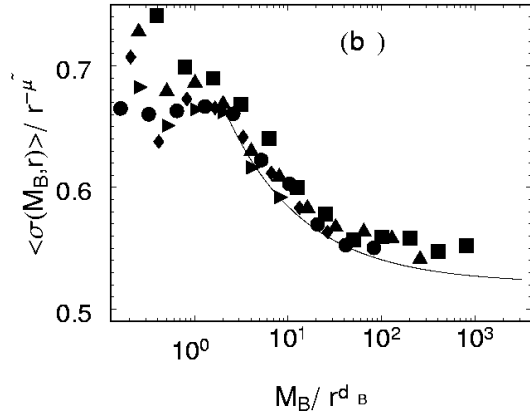
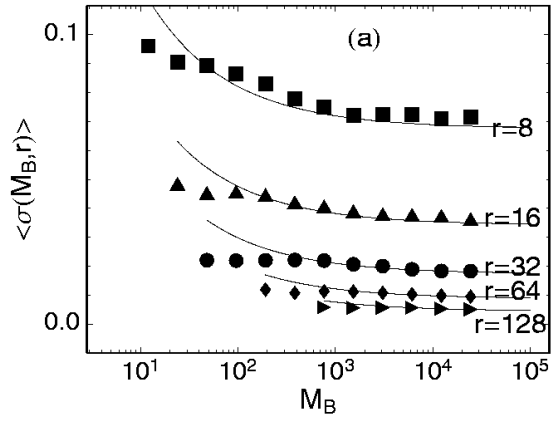


FIG. 2. Average conductance versus backbone mass. (a) Simulation results at the percolation threshold for  $r = 8, 16, 32, 64,$  and  $128$ , where  $r$  is the distance between the two sites  $A$  and  $B$ ; the adjacent lines are the theoretical results. For large  $r$ , the curves for the simulation results and the corresponding curves for the theoretical results coincide for large  $M_B$ . (b) Plots of scaled backbone conductance for  $r = 8, 16, 32, 64,$  and  $128$ , scaled in accordance with Eqs. (16) and (17). The solid line is a plot of Eq. (16) with parameters  $a$  and  $b$  chosen as  $0.9$  and  $6$  respectively to best fit the values for  $r = 128$  (right-pointing triangles). The collapse to this line for the lower values of  $r$  improves with increasing  $r$ . (c) Average conductance for  $r = 4$  for  $p = 0.50, 0.56,$  and  $0.60$ . For  $p = 0.56$ , the conductance as a function of  $M_B$  is not monotonic but rather has a minimum indicated by the arrow.

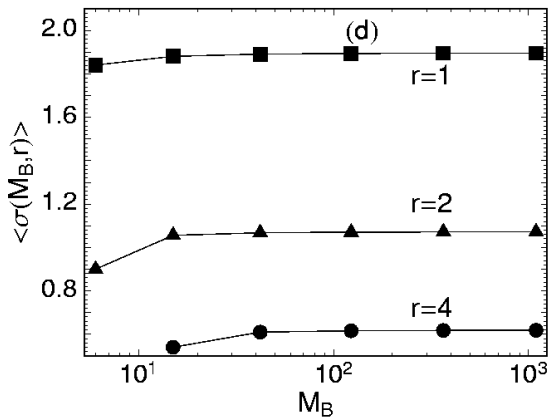
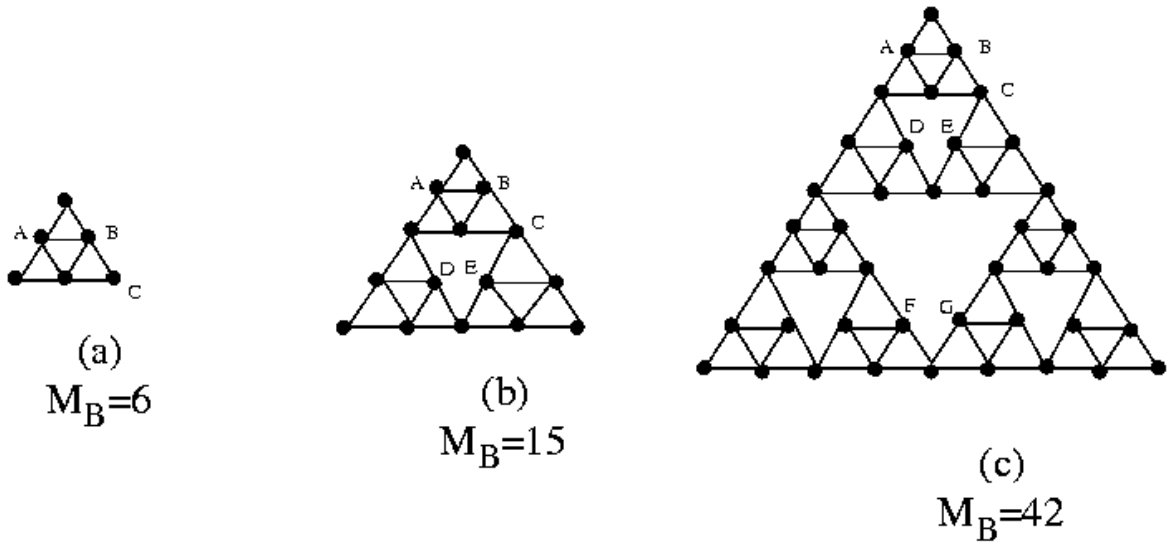


FIG. 3. (a)–(c) Three generations of the Sierpinski gasket. At each successive generation, there are two types of pairs of points: pairs which correspond to pairs in the previous generation and pairs which do not. For example, in the second generation the pairs AB and AC are present in the previous generation but the pair DE has no corresponding pair in the previous generation. Similarly, the pairs AB, AC, and DE in the third generation correspond to pairs in the second generation, but the pair FG does not. Because all points are multiply connected, the mass of the backbone between any two points in each generation is equal to the mass of the entire gasket. (d) Average conductance between all pairs of points separated by distance  $r$  on the Sierpinski gasket versus the gasket mass. The points correspond to successive generations of the Sierpinski gasket.

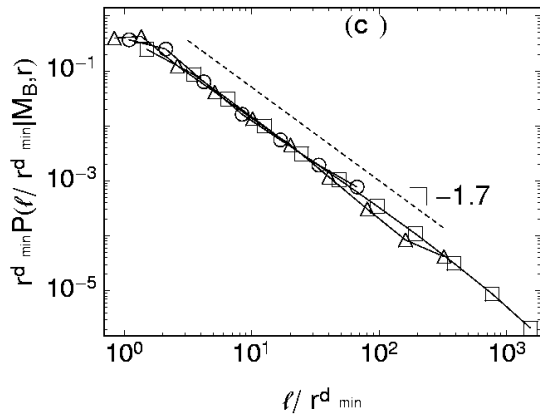
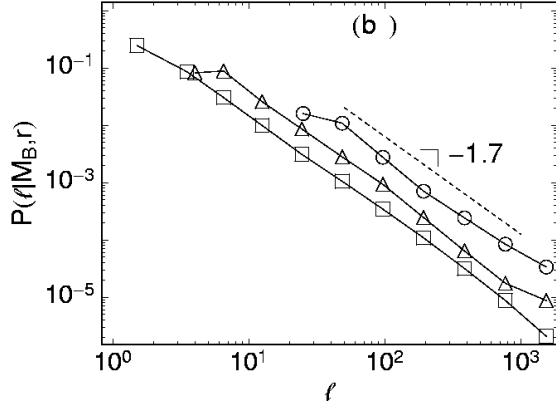
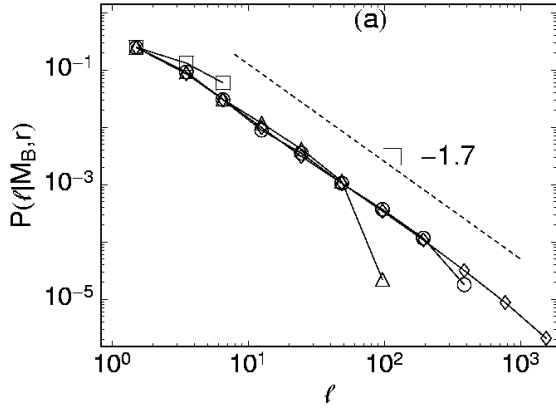


FIG. 4. Distribution of shortest paths between  $A$  and  $B$ . (a)  $P(\ell|M_B, r)$ , the probability that the length of the shortest path between two points separated by distance  $r$  is  $\ell$  for a given backbone mass,  $M_B$ . All plots are for  $r = 1$ , for values of  $M_B$  of 6 (squares), 96 (diamonds), 1536 (circles), and 24576 (triangles). The plots for the various  $M_B$  differ by the points at which they cut off. (b)  $P(\ell|M_B, r)$  for  $r = 1$  (squares), 4 (diamonds), and 16 (circles) for a single backbone size of 24576. (c) When scaled by  $r^{d_{\min}}$ , the plots collapse. The dashed line is constructed to have a slope of  $-1.7$ ; see Eq. (7).